

Dye tracing a jökulhlaup: I. Subglacial water transit speed and water-storage mechanism

Mauro A. WERDER,¹ Alexandre LOYE,^{1,2} Martin FUNK¹

¹ *Versuchsanstalt für Wasserbau, Hydrologie und Glaziologie (VAW), ETH Zürich, CH-8092 Zürich, Switzerland
E-mail: werder@vaw.baug.ethz.ch*

² *Institute of Geomatics and Risk Analysis, University of Lausanne, CH-1015 Lausanne, Switzerland*

ABSTRACT. We present results of an investigation of two jökulhlaups (glacial lake outburst floods) at Gornergletscher, Switzerland, using dye-tracer experiments and complementary hydrological measurements. Repeated dye injections into moulins showed that tracer transit speeds were larger after the lake had emptied, but when proglacial discharge was still high, than during the main phase of the jökulhlaup. This counter-intuitive finding was modelled by tracer retardation inside the injection moulin. This model, together with an estimate of the maximum time the tracer takes to transit the injection moulin, allows us to calculate bounds on the transit speed in the main drainage channel where the lake water flows. These results indicate that the main drainage channel transit speeds are indeed highest during the peak of the flood. Moreover, it is known from a previous study that water amounting to half of the lake volume is temporarily stored within the glacier during a Gornergletscher jökulhlaup. Our observations suggest that this process occurred via lateral spreading of water at the glacier bed.

INTRODUCTION

Jökulhlaups, also known as glacial lake outburst floods, commonly occur in glaciated regions around the world and present one of the greatest glacier-related hazards. Ice-dammed lakes tend to drain rapidly once an initial drainage pathway has been established. The jökulhlaup starts and proceeds either by melt enlargement of the drainage channel or by flotation of the ice dam (Tweed and Russell, 1999; Roberts, 2005). Jökulhlaups represent a unique test piece for theories of the evolution of the subglacial drainage system (e.g. Nye, 1976; Spring and Hutter, 1982; Clarke, 2003). They allow the study of the response of the glacial drainage system and also of the entire glacier to a large basal perturbation (e.g. Björnsson, 1998; Sugiyama and others, 2007; Bartholomaus and others, 2008; Stearns and others, 2008). Many aspects of jökulhlaups are still poorly understood, and two large field campaigns were conducted recently to collect more experimental data. Anderson and others (2003) studied the jökulhlaups of Kennicott Glacier, Alaska, USA, and we studied the jökulhlaups of Gornergletscher, Switzerland (Huss and others, 2007; Sugiyama and others, 2007, 2008; Walter and others, 2008, 2009).

The glacial drainage system changes on spatial and temporal scales which are far smaller than those of most other relevant glaciological processes. This fact and the general inaccessibility of the glacial drainage system make its experimental investigation a formidable task. Tracer experiments are one of the few experimental methods that allow the sub- and englacial drainage system to be probed. Other methods include measurements of subglacial water pressure in boreholes, slug tests, discharge into and out of the glacier, and geophysical methods, such as radar and seismology. Dye-tracer investigations on glaciers range from studies of the aquifer in the firn (e.g. Lang and others, 1981) to studies resolving the highly dynamic nature of the drainage system on an hourly timescale (e.g. Schuler and others, 2004). However, only two dye-tracer

studies on aspects of jökulhlaups have been published to date: Aschwanden and Leibundgut (1982), who, like us, investigate a Gornergletscher jökulhlaup, and Fisher (1973). Tracer experiments yield information integrated over the entire flow path of the water on its passage through the glacier. This makes their quantitative evaluation difficult, as most established theories of the glacial drainage system describe only a part of the tracer flow path. In particular, models of jökulhlaups describe the flow of the lake water in the R channel connecting the lake to the proglacial stream (Fowler, 1999; Clarke, 2003), ignore the rest of the glacial drainage system and thus neglect the influence of the outburst on the drainage of the supraglacial meltwater. However, it is this meltwater which is usually traced and its whole flow path needs to be taken into account to interpret tracer experiments correctly.

From 2005 to 2007, we conducted more than 200 tracer experiments to study the yearly jökulhlaups on Gornergletscher. The aim was to investigate the reaction of the glacial drainage system to the large perturbation caused by jökulhlaups. The results and interpretation of some of these tracer experiments are presented here and in the companion paper (Werder and Funk, 2009). The present paper focuses on the influence of the jökulhlaup on the whole glacial drainage system in 2005 and 2007, when the lake was drained as an intense subglacial jökulhlaup. We first define our terminology and give a brief overview of the field site, the experimental methods and the techniques used for data processing. We introduce a simple lumped-element model to estimate the influence of englacial water flow on the tracer passage before it meets up with the lake water in the main subglacial drainage channel. Measurements of subglacial water pressure head, lake and proglacial discharge are presented to complement the results of tracer experiments conducted before, during and after the jökulhlaups using moulins situated down-glacier from the lake. Taking the measured transit speeds, we use the lumped-element model to derive a range of main drainage channel

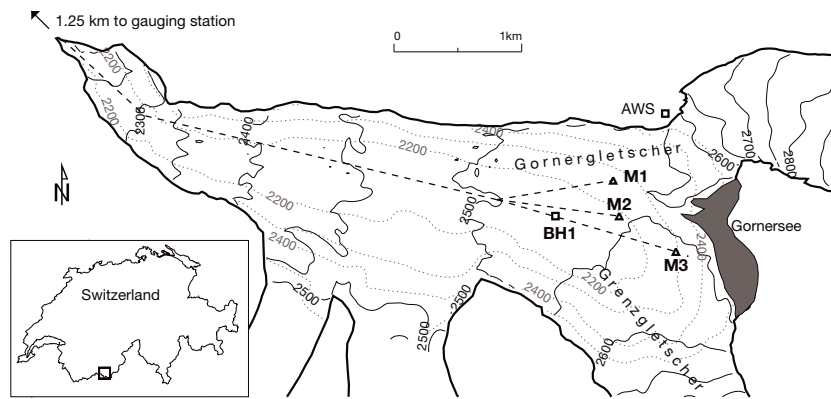


Fig. 1. Map of the tongue of Gornergletscher with solid contours of surface elevation and dotted contours of bed elevation. The locations of the moulin used for the tracer injections are marked by triangles labelled M1, M2 and M3. The dashed lines indicate the path used to compute the transit distance of each moulin. The subglacial water pressure was measured in a borehole (BH1). The position of the automatic weather station is marked (AWS).

transit speeds during the jökulhlaup. The companion paper (Werder and Funk, 2009) focuses, not on the whole drainage system, but on the development of the lake drainage channel during the onset of the jökulhlaup in 2006. On the first 1.5 days of this jökulhlaup we were able to inject tracer into the lake outlet, and thus measure the transit speed of the lake water, allowing, for the first time, a jökulhlaup model (Clarke, 2003) to be tested not only against lake discharge but also against flow speeds inferred from measurements.

TERMINOLOGY

In order to describe and discuss the tracer experiments and the accompanying model, a few concepts need to be elucidated and terms defined. We assume that the tracer and the water travel at the same velocity, so the following definitions apply equally to both.

The time interval between the passage of the maximum concentration of the tracer cloud at two locations is the *residence time*, t (sometimes called dominant residence time). The shortest possible horizontal distance between those two locations is the *transit distance*, \hat{l} , leading to the *transit speed* as the ratio of the transit distance and residence time ($\hat{v} = \hat{l}/t$). If not specified further, the two locations are, by implication, the injection and detection sites. The actual distance travelled by the tracer is the *flow path length*, l . Of course, the time to traverse the *flow path* is also the residence time. Note that the flow path length will, in general, be larger than the transit distance, due to the additional vertical distance covered and to the geometry and sinuosity of the flow path. This means that the transit speed is a lower bound on the mean, channel cross-section averaged *flow speed*, $v = l/t$.

Note that hydraulic models, like the one presented here, use the flow path length and calculate flow speed, not transit distance and speed, so care must be taken when comparing experimental and model results. The reason for introducing the transit speed and not exclusively using the residence time is that it makes it possible to compare results from experiments using different injection sites with different transit distances. Our definition of transit speed is identical to the term 'dominant effective flow velocity' that is sometimes used (Käss, 1998); we decided to introduce the new terms transit distance and speed to make their close association clear and distinguish them from the flow path length and

flow speed. Furthermore, note that the *mean* residence time is the time interval from injection until half the tracer cloud has passed the detection site, and will be longer than the residence time, as we define it, in the (usual) situation when storage-release processes occur.

FIELD SITE

Gornergletscher is the second largest glacier in the Alps, with an area of $\sim 60 \text{ km}^2$. It covers altitudes from 4600 down to 2200 m a.s.l. and has a maximum length of 14 km (Huss and others, 2007). Gornersee is an ice marginal lake located in the confluence area of the two main tributaries Gorner- and Grenzgletscher (Fig. 1). The lake has an elevation of 2530 m a.s.l. and lies 5.25 km up-glacier of the terminus. The maximum ice thickness of 450 m is found 1 km down-glacier of the lake (Sugiyama and others, 2008). Gornersee fills every spring and drains in summer, normally as a subglacial jökulhlaup, but supraglacial overspill has also been observed. In past years the maximum volume of the lake basin has been estimated at $\sim 4.5 \times 10^6 \text{ m}^3$. However, the lake does not always fill up completely. Peak discharge from the lake is $\sim 20 \text{ m}^3 \text{ s}^{-1}$ and in the proglacial stream it is $\sim 40 \text{ m}^3 \text{ s}^{-1}$, of which about half is meltwater and the rest is from the lake. Peak inflow of meltwater into the lake is $\sim 5 \text{ m}^3 \text{ s}^{-1}$. The jökulhlaup lasts for ~ 2 to 7 days, depending on the lake volume and the exact outburst mechanism (Huss and others, 2007). The lake takes about 3 weeks to empty if it drains by supraglacial overspill into a moulin. Two features which set Gornersee jökulhlaups apart from most others studied so far are that the lake is small compared to the glacier damming it, and that peak proglacial discharge during the jökulhlaup is only about twice the discharge due to melt.

METHODS

We used two fluorescent dyes, Uranine (UR) and Rhodamine WT (RWT), for tracer injections. Both are suited to glacial environments and can be used simultaneously. Injections were conducted by hand into selected meltwater streams just before they entered a moulin. The time required for injection was always short compared to the residence time, so for data evaluation we can assume instantaneous injections. All injections were carried out at 1400 h local

daylight savings time (CEST; UTC+2) to keep the boundary conditions as constant as possible. We present results of 24 from a total of 101 injections conducted daily in 2005 and less frequently in 2007.

Tracer injections were performed using three moulins (M1, M2, M3); their positions are marked in Figure 1. M1, used in 2005, was located 600 m down-glacier from the lake. During the measurement period, the daily discharge maximum of M1 was $\sim 0.5 \text{ m}^3 \text{ s}^{-1}$. M2, used in 2007, was situated 500 m down-glacier from the lake, probably closer to the main subglacial drainage channel (where the bulk of the glacier discharge flows) than M1 (see Werder and Funk, 2009, for a discussion of the location of the main subglacial drainage channel). M2 carried a discharge comparable to M1. M3, also used in 2007, was located 200 m from the lake, just on the down-glacier edge of the lake dam on the Grenzgletscher side. It was substantially smaller than M1 and M2, attaining an estimated daily discharge maximum of $\sim 0.05 \text{ m}^3 \text{ s}^{-1}$ during the measurement period. M1, M2 and M3 have transit distances of 6, 6 and 6.5 km, respectively. The corresponding paths are shown as a dashed line in Figure 1 for each moulin.

The dye was detected $\sim 1.25 \text{ km}$ downstream of the terminus at the water-gauging station of Grande Dixence SA. RWT concentration was measured using a Turner 10-AU flow-through fluorometer that allows continuous measurements. Water was fed through the fluorometer by a pump submerged in the pool of the gauging station. The UR concentration was measured using a BackScat submersible fluorometer, at the same location, also allowing continuous dye detection. Both fluorometers were calibrated using the water of the proglacial stream. The detection limit for the two dyes was $\sim 0.3 \text{ ppb}$, but for good signal-to-noise ratio a peak concentration $> 3 \text{ ppb}$ was desirable. The conducted experiments had an average fraction of recovered dye mass of ~ 0.5 , and thus a considerable amount of dye was lost somewhere in the glacial drainage system which could interfere with subsequent experiments. However, the main concentration peaks of the presented experiments are high and narrow enough that dye released from previous experiments is unlikely to modify them significantly. Furthermore, on days when no tracer experiments were conducted, the fluorometers continued to run and did not register any release events which were clearly above the background noise.

The proglacial discharge was measured by Grande Dixence SA at the gauging station with an error of 10%. The lake discharge was derived from the measured lake level and water input into the lake which was calculated by a melt model driven by temperature data from the automatic weather station (Fig. 1; see Huss and others, 2007, for details). The error in the lake discharge was estimated to be 20%. For 2005, we present subglacial water pressure-head data measured in a borehole drilled to the bed (Fig. 1). Subglacial water pressure data are not available for 2007.

Data processing

Most of the processing of the tracer data follows Schuler and others (2004). The continuous time series recorded by the fluorometers were segmented into pieces corresponding to the individual injections. No breakthrough curves of the presented experiments were overlapping. To characterize the breakthrough curves, an advection–dispersion model with storage term (ADSM) was fitted to them (Van Genuchten and Wierenga, 1976; De Smedt and others, 2005). The equations

for this model in a glaciological setting are given by Schuler and others (2004). The fitting was performed using the CXTFIT2.0 program, which is available from the US Salinity Laboratory (Toride and others, 1999). The program requires as input the tracer concentration time series, transit distance and initial guesses for the fitting parameters. The ADSM returns four parameters estimating the mean transit speed, the hydrodynamic dispersion, D , the fraction of mobile water, β , and the exchange rate between mobile and immobile water, ω . We present the transit speed, and not the mean transit speed, \hat{v} , as returned by the ADSM, as the former is more readily compared to results from our hydraulic model. D is a measure of the width of the rising part of the breakthrough curve (see Fountain, 1993; Schuler and Fischer, 2003). D depends mostly on the intensity of turbulent mixing: a boulder-strewn river bed leads to more dispersion than a smooth bed. The two storage-release terms, β and ω , are measures of the size of the tail of a breakthrough curve. In the case of a bad fit of the ADSM to the breakthrough curve, we omitted the estimated parameters in the figures. The fraction of returned tracer mass, M , was obtained by integrating the tracer concentration multiplied by the proglacial discharge divided by the injected tracer mass. Our interpretation rests on the transit speed, \hat{v} , D , β and M ; thus the presentation of ω is omitted.

Lumped-element model

We envisage that surface water entering a moulin will first have to flow englacially, and possibly also subglacially, through a tributary flow path before it reaches the main drainage channel, where the bulk of the meltwater, and also the lake water, flows. This main drainage channel is likely to be located at the glacier bed (Fountain and Walder, 1998) and consists of a semicircular channel incised into the ice, known as the R channel (Röthlisberger, 1972). Here we set up a model to simulate the flow of the water through a moulin and a subsequent tributary R channel before it reaches the main drainage channel. The ratio of the water volume to the discharge of a moulin is large, so water flow speed in the moulin is slow. The water volume contained in the moulin is dictated by the filling height of the moulin, which is equal to the subglacial water pressure head. This leads to a water flow speed inside the moulin which is inversely proportional to the subglacial water pressure. This is very different to water flow in R channels, where flow speed increases with increasing subglacial water pressure gradient. This process of water retardation inside a moulin is called inflow modulation (Kohler, 1995; Nienow and others, 1996; Schuler and others, 2004). We model the inflow modulation using the simple and elegant lumped-element approach (Clarke, 1996). This model is then used to interpret the measured transit speeds of the experiments conducted using M1.

The model is shown schematically in Figure 2, and consists of a moulin element connected to an R-channel element. The moulin element has a constant cross-sectional area, S_m , a filling height, h_0 , and is fed by a time-varying input discharge, Q . The moulin element is connected via an R-channel element to the main drainage channel. The R channel has a circular cross-section, a resistance, R , and carries a discharge, Q_0 . We did not simulate the main drainage channel; instead we used measured subglacial water pressure head as the boundary condition, h_{out} , at the lower end of the R-channel element.

Table 1. Constants used in the lumped-element model

Constant	Variable	Value
Ice-flow exponent	n	3
Latent heat of fusion	L	333.5 kJ kg^{-1}
Pressure-melting coefficient	C_t	$7.5 \times 10^{-8} \text{ K Pa}^{-1}$
Specific heat capacity of water	C_p	$4180 \text{ J kg}^{-1} \text{ K}^{-1}$
Gravitational acceleration	g	9.8 m s^{-2}
Density of water	ρ_w	1000 kg m^{-3}
Density of ice	ρ_i	900 kg m^{-3}
Ice-flow constant	B	$5.3 \times 10^{-24} \text{ Pa}^{-n} \text{ s}^{-1}$

Following Clarke (1996), the model is described by the system of equations:

$$\frac{dh_0}{dt} = \begin{cases} 0 & \text{if } h_0 \geq h_{\max}, Q \geq Q_0 \\ \frac{Q-Q_0}{S_m} & \text{otherwise} \end{cases} \quad (1)$$

$$h_0 - h_{\text{out}} = RQ_0^2 \quad (2)$$

$$\frac{dS_c}{dt} = C_1 Q_0 (h_0 - h_{\text{out}}) / l_c - C_2 (h^* - \bar{h})^n S_c, \quad (3)$$

where $C_1 = (1 - \rho_w C_p C_t) \frac{\rho_w g}{\rho_i L}$ and $C_2 = 2B \left(\frac{\rho_w g}{n} \right)^n$ are constants, h_{\max} is the maximum filling height of the moulin, S_c is the channel cross-section, $h^* = \rho_i h_i / \rho_w$ is the pressure head corresponding to flotation pressure above the channel, $\bar{h} = \frac{1}{2}(h_0 + h_{\text{out}})$ is the mean pressure head in the channel and l_c is the channel (flow-path) length. The values used for the physical constants are given in Table 1.

Equation (1) relates the time evolution of the filling height of the moulin to input and output discharge. Note that this assumes that water entering the moulin reaches the filling level, h_0 , immediately. This is a good approximation, as flow speed is fast in the very steep shaft. The R channel is modelled as a turbulent flow resistor (Equation (2)). The time evolution of the cross-sectional area of the R channel is given by Equation (3), where the first term describes channel enlargement through dissipation of potential energy and the second term describes channel closure by ice creep. The resistance, R , is calculated from S_c , assuming a circular cross-section, with

$$R = 2^{4/3} \pi^{2/3} n_{\text{man}}^2 l_c S_c^{-8/3}, \quad (4)$$

using the Gauckler–Manning–Strickler formulation with Manning roughness, n_{man} (Chow and others, 1988). This system of differential algebraic equations was solved with the Matlab™ ode15s solver.

The modelled residence time in the moulin element is approximated by

$$t_m = \frac{S_m}{Q_0} h_0, \quad (5)$$

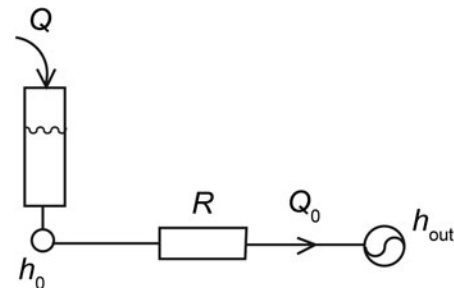


Fig. 2. Diagram of the lumped-element model used to simulate transit speed. The moulin element (left) is fed by the input discharge, Q , and has a filling height h_0 . The R-channel element (middle) has resistance R and discharge Q_0 . The lower boundary condition (right) is prescribed by the time-varying pressure head, h_{out} .

assuming constant discharge conditions during the passage of the tracer. Similarly, the modelled residence time in the R-channel element is approximated by

$$t_c = \frac{S_c}{Q_0} l_c, \quad (6)$$

and the sum

$$t = t_m + t_c \quad (7)$$

is the modelled residence time of moulin and tributary channel, i.e. the time it takes the tracer to reach the main drainage channel. Assuming the model is correct, the transit speed in the main drainage channel, \hat{v}_{main} , can be calculated as

$$\hat{v}_{\text{main}} = \frac{\hat{l}_{\text{main}}}{t_{\text{tot}} - t}, \quad (8)$$

where t_{tot} is the measured residence time and \hat{l}_{main} is the transit distance of the main drainage channel.

RESULTS

For both years, 2005 and 2007, we first outline the general course of events during the jökulhlaup (Table 2) and then focus on the results of the tracer experiments. To help the presentation, we divide the time span of both jökulhlaups into three phases: (1) the onset phase, when the proglacial discharge had not yet increased; (2) the main phase, when lake and proglacial discharge was high; and (3) the terminating phase, when the lake had emptied but proglacial discharge was still high. In the figures displaying the results, these three phases are shaded with different levels of grey (Figs 3–6). In the last part of this section, we present the results of running the lumped-element model with data from 2005 to establish bounds on water transit speed in the main drainage channel.

Table 2. Comparison of the key observations of the lake drainages in 2005 and 2007

Year	Lake drainage characteristics	Date of onset	Duration days	Peak lake discharge $\text{m}^3 \text{ s}^{-1}$	Peak proglacial discharge $\text{m}^3 \text{ s}^{-1}$	Lake volume 10^6 m^3
2005	Subglacial	10 June	6	10	20	1.5
2007	Sub- and supraglacial	4 July	8	15	27	3.7

Observations in 2005

The lake was filled to one-third of its potential volume when the jökulhlaup began (10 June). The lake discharge increased progressively until the lake was empty on 15 June (Fig. 3e; phases 1 and 2). Hydrograph separation (Huss and others, 2007) showed that lake water was exiting the glacier between 13 and 15 June (phases 2 and 3). In phase 1, the daily minima of the subglacial water pressure head (Fig. 3f) increased until, during phase 2, the water pressure remained at flotation level throughout the day. In phase 3 the pressure dropped abruptly and diurnal fluctuations recommenced the day after, albeit with a larger amplitude than before the jökulhlaup. The transit speed from the experiments conducted using M1 increased evenly throughout the measurement period (Fig. 3a), apart from a local maximum on 15 June, during phase 3. The corresponding residence time of the injection on 15 June was 30 min shorter than the residence time of the injection on 14 June. The injection on 12 June (phase 1), during the onset of the jökulhlaup, produced a high dispersion, D , combined with a low fraction of mobile water, β . The fraction of returned tracer mass, M , peaked at 0.8 during phase 2 and was otherwise ~ 0.4 .

Observations in 2007

The lake was filled to its maximum volume when its shore reached a moulin on 4 July. It spilled over into this moulin and discharge stayed low until subglacial lake drainage initiated on 7 July. The main outburst happened during the next 2 days, when the bulk of the lake water drained into a crevasse which had opened at around mid-height of the lake basin. During the main outburst the peak lake discharge of $15 \text{ m}^3 \text{ s}^{-1}$ was attained. On 9 July, the lake level had dropped to the height of this crevasse and drainage occurred again by supraglacial overspill. During the next 5 days subglacial drainage and supraglacial overspill alternated twice again until the lake was empty on 15 July. This caused the lake discharge to fluctuate considerably (Fig. 4e and j).

The proglacial discharge rose to $27 \text{ m}^3 \text{ s}^{-1}$ at the end of the main outburst and less during the subsequent subglacial drainage periods.

Figure 4a–d show the results of injections into M2. Before and during phases 1 and 2 of the jökulhlaup, the transit speed was $\sim 0.8 \text{ m s}^{-1}$. The injection on 13 July (phase 3) produced the maximum transit speed of 1.3 m s^{-1} . The transit speed of the injection after the jökulhlaup was slightly lower at 1.2 m s^{-1} . The experiments yielded a decreased D during the later stage of phase 2 and during phase 3, and an increased D after the jökulhlaup. β was high throughout and M peaked in phase 2.

Prior to the jökulhlaup in 2007, the injection using M3 on 2 July resulted in a transit speed of 0.6 m s^{-1} (Fig. 4f–i). In phase 2, there was a local maximum of transit speed (0.8 m s^{-1}) obtained from the injection on 10 July. The global maximum of the measured transit speed of 1.1 m s^{-1} was attained 2 days after phase 3, on 15 July. One week later, the transit speed dropped back to 0.7 m s^{-1} . D had a maximum on 10 July coinciding with the local maximum of the transit speed and the minimum of β (phase 2). M was 0.7 before and dropped to 0.1–0.4 during the jökulhlaup. Figure 5 shows the breakthrough curves from experiments using M3. The experiment on 9 July (phase 2) returned the lowest M (0.1) and its breakthrough curve was very spread out and could not be fitted by the ADSM.

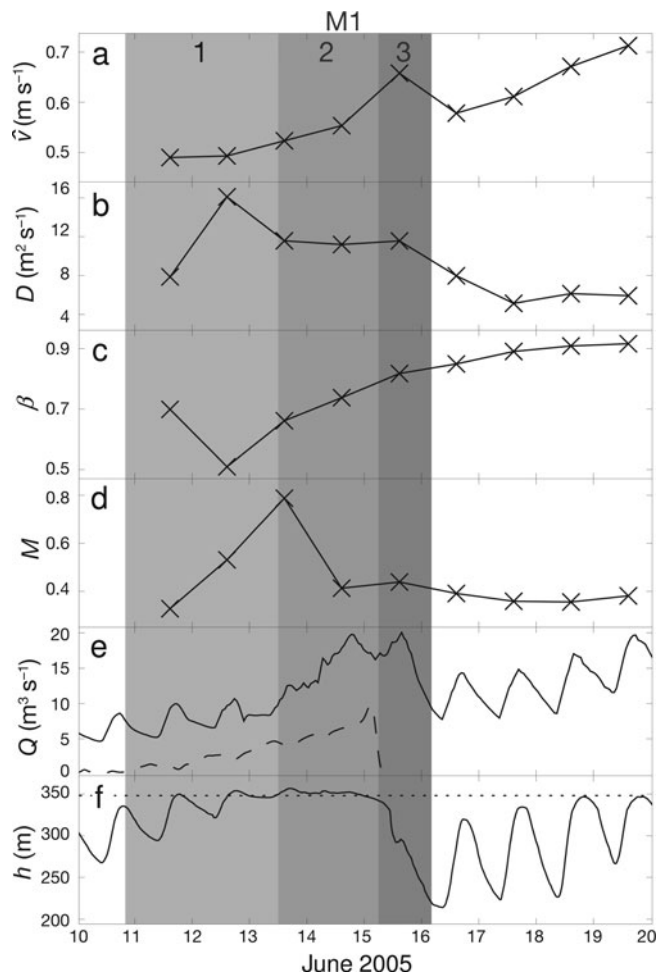


Fig. 3. Results from daily injections into moulin M1, hydrographs and subglacial water pressure head during and after the jökulhlaup in 2005. The crosses are plotted at the time of injection. (a) Transit speed, \hat{v} ; (b) dispersion, D ; (c) fraction of mobile water, β ; (d) fraction of returned tracer mass, M ; (e) lake (dashed curve) and proglacial discharge (solid curve); and (f) subglacial water pressure head in borehole BH1 (dotted line corresponds to flotation level). The three phases into which the jökulhlaup was divided are shown in different shades of grey.

Model results

We ran the lumped-element model (Fig. 2) to investigate the influence of inflow modulation on the results of injections into M1 from 7 to 17 June 2005. The model calculates the time to reach the main drainage channel, t (Equation (7)), and the transit speed in the main drainage channel, \hat{v}_{main} (Equation (8)). For the lower boundary condition, h_{out} , we use the subglacial water pressure-head data from BH1 (Fig. 3f). (The lack of corresponding pressure data for 2007 was the reason why this model is only applied to 2005.) For the upper boundary condition, we assumed a sinusoidally varying discharge, Q , into the moulin element having an amplitude $0.26 \text{ m}^3 \text{ s}^{-1}$, a mean value $0.30 \text{ m}^3 \text{ s}^{-1}$ and a maximum at 1400h. Table 3 summarizes the parameters used for the model. The length of the connection channel, $l_c = 500 \text{ m}$, was chosen equal to the horizontal distance between M1 and BH1. This is the shortest conceivable connection channel length. The only data available to fit the model were the observed decrease of the residence time of 30 min from 14 to 15 June. For the first model run (Mod1), we chose the

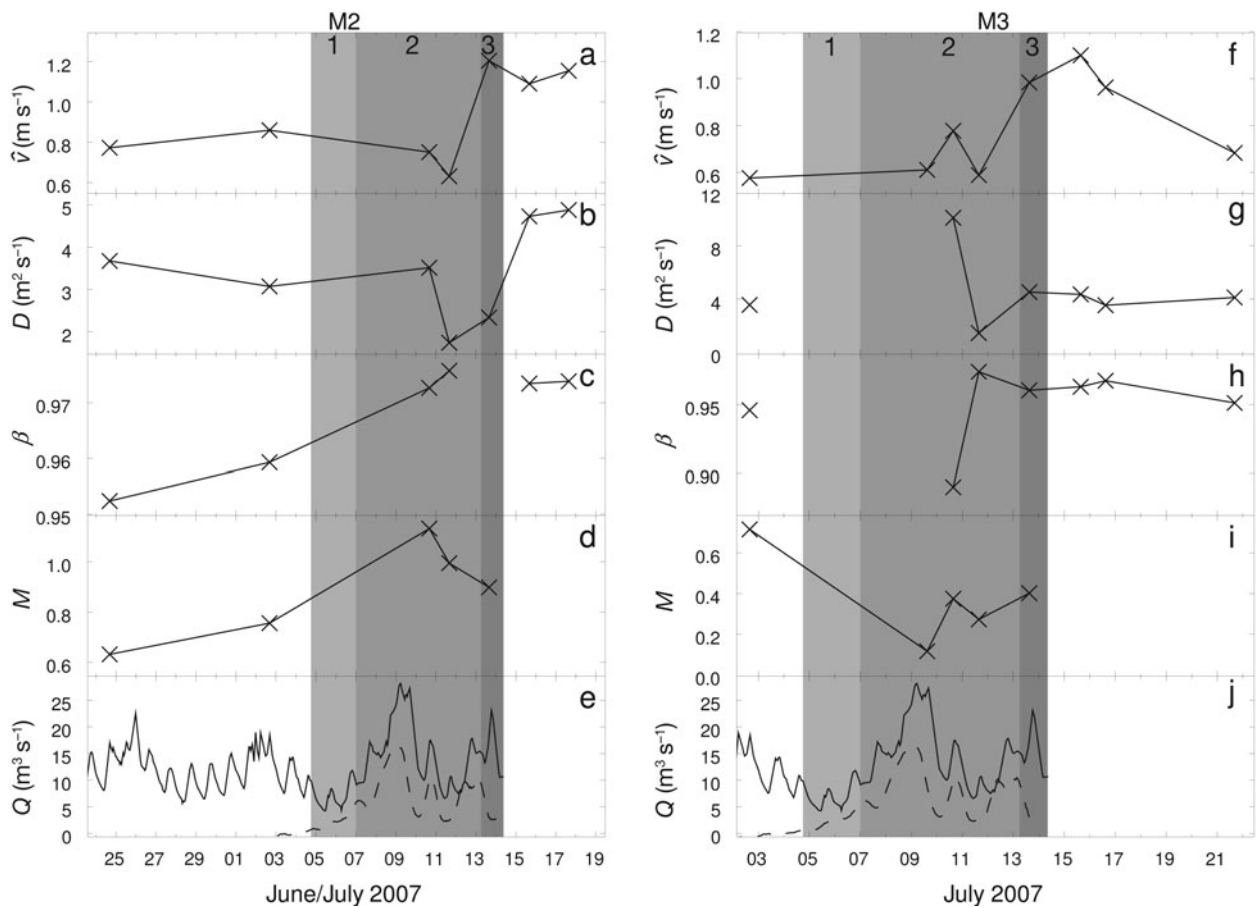


Fig. 4. Results from injections into moulin M2 (left) and moulin M3 (right) and hydrographs for the jökulhlaup in 2007. The crosses are plotted at the time of injection. (a, f) Transit speed, \hat{v} ; (b, g) dispersion, D ; (c, h) fraction of mobile water, β ; (d, i) fraction of returned tracer mass, M ; (e, j) lake (dashed curve) and proglacial discharge (solid curve). The three phases into which the jökulhlaup was divided are shown in different shades of grey. Missing points indicate that the ADSM could not be fitted (c, g, h) or that the proglacial discharge measurement was broken (d, e, i, j).

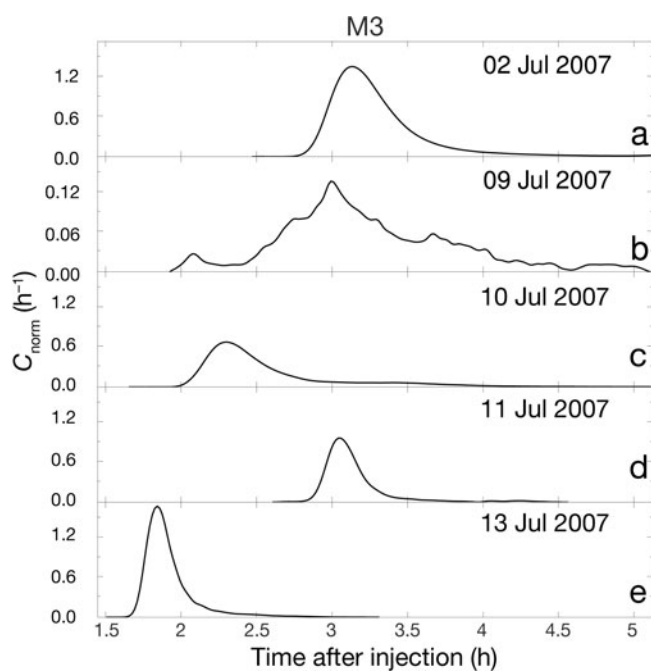


Fig. 5. Breakthrough curves from injections into M3 (cf. Fig. 4) normalized by dividing the tracer mass flux through the injected mass, C_{norm} . The label gives the injection date. All the plots have the same y-axis scale except (b) which has one that is 10 times smaller.

cross-sectional area of the moulin, $S_m = 15.5 \text{ m}^2$, such that t also decreased by 30 min from 14 to 15 June (Fig. 6a and b). The 30 min residence time difference is a probably a lower bound, as elucidated below, so we performed a second model run (Mod2) with a 1.5 times larger cross-sectional area of the moulin, $S_m = 23 \text{ m}^2$, (Fig. 6c and d) which resulted in a t decrease of 43 min from 14 to 15 June. The model has other free parameters (l_c and n_{man}), but there were not enough field data available to constrain these, so they are set to physically reasonable values. This means that the calculated times to reach the main drainage channel, t , are only relative values, i.e. the whole time series of the t may be shifted by a constant offset (cf. Fig. 6a and c). Bounds of

Table 3. Parameters of the lumped-element model

Parameter	Variable	Value
Channel flow path length	l_c	500 m
Transit distance of main drainage channel	\hat{l}_{main}	5500 m
Moulin cross-sectional area	S_m	15.5 and 23.0 m^2
Ice thickness	h_{ice}	400 m
Maximum filling height	h_{max}	400 m
Manning roughness factor	n_{man}	$0.033 \text{ m}^{-1/3} \text{ s}$

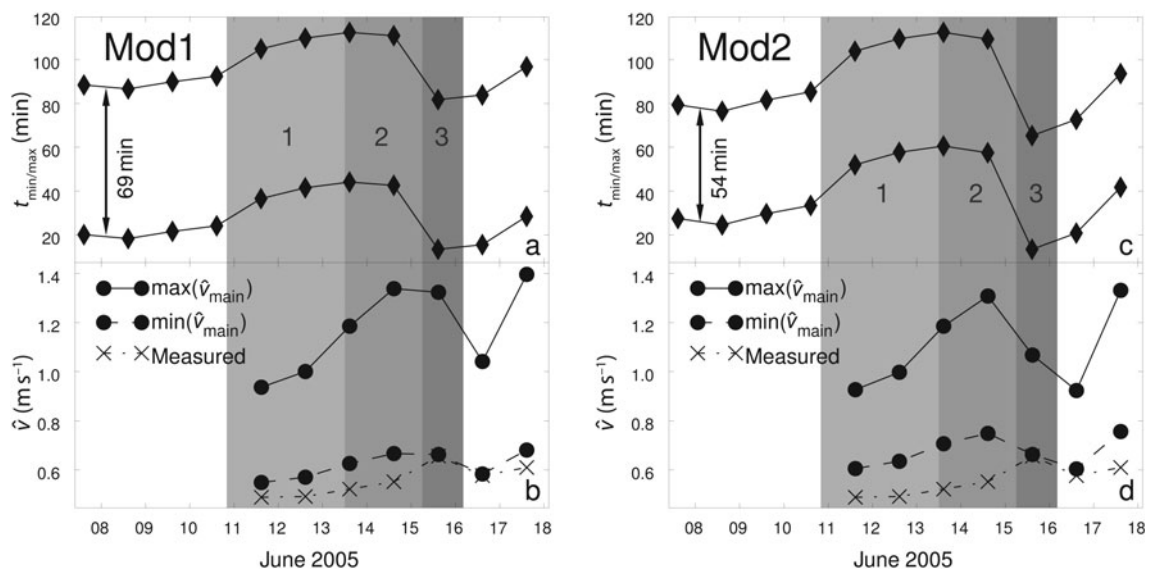


Fig. 6. Results of model run Mod1 ($S_m = 15.5 \text{ m}^2$; a, b) and Mod2 ($S_m = 23 \text{ m}^2$; c, d). (a, c) Minimum and maximum modelled time ($t_{\min/\max}$) to reach the main drainage channel at 1400 h. (b, d) Measured (total) transit speed, \hat{v} , and the derived bounds on the transit speed in the main drainage channel (\hat{v}_{main} , Equations (8–10)). The three phases into which the jökulhlaup was divided are shown in different shades of grey.

the minimum and maximum value of t can be obtained by the following argument: The calculated residence time in the connection channel (t_c , Equation (6)) stayed fairly constant at ~ 7 min and we assumed that the residence time in the moulin (t_m , Equation (5)) was at least as long (the moulin was 400 m deep), so the minimum t was at least 14 min (i.e. $\min(t) > 14$ min). The experiment on 24 June 2005 yielded the shortest measured residence time of 113 min, so we assumed that the maximum t is smaller than 113 min (i.e. $\max(t) < 113$ min). The two time series t_{\min} and t_{\max} we defined as containing the smallest and largest possible values of t , respectively,

$$\min(t_{\min}) = 14 \text{ min} \quad (9)$$

$$\max(t_{\max}) = 113 \text{ min.} \quad (10)$$

For Mod1 this resulted in a shift of 69 min with respect to each other (Fig. 6a), and of 54 min for Mod2 (Fig. 6c). The minimum and maximum transit speeds in the main drainage channel, $\min(\hat{v}_{\text{main}})$ and $\max(\hat{v}_{\text{main}})$ in Figure 6b and d, could now be calculated using Equation (8), substituting t_{\min} and t_{\max} for t .

In the Mod1 model run, the minimum/maximum time to reach the main drainage channel, $t_{\min/\max}$ (Fig. 6a), increased by 20 min in phases 1 and 2 and then dropped by 30 min by phase 3 (as required by our fitting procedure). The transit speed in the main drainage channel $\max/\min(\hat{v}_{\text{main}})$ (Fig. 6b), calculated from $t_{\min/\max}$ and the measurements (Equation (8)), increased during phases 1 and 2, stayed level in phase 3 and decreased the day after. In the Mod2 model run, $t_{\min/\max}$ (Fig. 6c) increased by 30 min during phases 1 and 2 (10 min more than in Mod1) and dropped by 43 min by phase 3 (13 min more than in Mod1); \hat{v}_{main} (Fig. 6d) increased throughout phases 1 and 2 and peaked at the end of phase 2, decreased in phase 3 and had its minimum the day after.

The maximum \hat{v}_{main} was 1.34 m s^{-1} for both models, as dictated by Equations (10) and (8). The measured transit speed (i.e. between injection and detection) was lower than

the calculated transit speed in the main drainage channel, \hat{v}_{main} , in both models, as the minimum time spent to reach the main drainage channel was greater than zero (14 min, Equation (9)).

DISCUSSION

We infer from the steadily increasing transit speeds resulting from injections into M1 (Fig. 3a) that during the jökulhlaup in 2005 the glacial drainage system was in its transition phase from the winter to the summer regime (Werder, 2009). This transition is a gradual process and progresses up-glacier as temperatures rise (Hubbard and Nienow, 1997). Superimposed on the steady increase of transit speed was a maximum on 15 June 2005, in phase 3 of the jökulhlaup. The transit speed of this maximum is 0.1 m s^{-1} larger than would be expected from an uninterrupted steady increase in the transit speed. The maximum occurred not at the time of highest lake discharge (phase 2), but after the lake had drained (phase 3).

In 2007 the jökulhlaup had a greater impact on the results of the tracer experiments than in 2005. The injection into M2 on 13 July yielded a transit speed of 1.2 m s^{-1} , twice the transit speed of the injection 2 days before. Similarly, an increase from 0.6 to 1.1 m s^{-1} was observed in the experiments using M3. This greater influence is probably due to three factors. Firstly, moulins M2 and M3 were situated closer to the likely drainage path of the lake than M1. Secondly, the jökulhlaup was larger in 2007 ($15 \text{ m}^3 \text{ s}^{-1}$ peak outflow) than in 2005 ($10 \text{ m}^3 \text{ s}^{-1}$). Thirdly, during the jökulhlaup in 2007 the drainage system was in a steady summer configuration, whereas the ongoing winter–summer transition of the drainage system in 2005 possibly masked the effects of the jökulhlaup. The timing of the maximum transit speed recorded from injections using M2 and M3 was similar to 2005; the maxima did not occur during peak lake discharge but afterwards. The transit speeds resulting from injections into M3 showed two maxima, the first one after

the main lake discharge event and the second, larger one after the lake had drained completely.

In both 2005 and 2007, the maximum transit speed occurred after the lake had emptied (phase 3) and not during the peak of the jökulhlaup (phase 2). We explain this counter-intuitive behaviour by tracer retardation inside the injection moulin. The effects of this so-called inflow modulation on the results of the experiments conducted using M1 (2005) were simulated with model runs Mod1 and Mod2 (Fig. 6). In both model runs, the calculated time to reach the main drainage channel, t (Equation (7)), was longer during phases 1 and 2 of the jökulhlaup than before and after them (Fig. 6a and c), because the tracer was delayed due to the higher filling level of the moulin caused by the high subglacial water pressure. t increases enough during phases 1 and 2 to mask the effects of the jökulhlaup on the measured transit speed; however, the calculated transit speed in the main drainage channel (\hat{v}_{main} , Equation (8)), increases during phase 1 and, in particular, phase 2, as would be expected (Fig. 6b and d). Note that for Mod1, values for \hat{v}_{main} at the end of phase 2 and in phase 3 were identical due to our fitting procedure, in which we adjusted S_m such that the measured residence time difference between 14 and 15 June was attained. In reality, it is likely that the actual \hat{v}_{main} was lower on 15 June, due to the following argument. The subglacial water pressure head in BH1 was 350 m on 14 June and 290 m on 15 June at 1400 h. On both days, roughly the same discharge ($20 \text{ m}^3 \text{ s}^{-1}$) was flowing at 1400 h in the main drainage channel, but on 15 June with a lower pressure differential. Hence, the main channel cross-sectional area must have been larger on 15 June to reduce frictional losses, and this means that the flow speed in the main channel was lower on 15 June. Thus, the estimated S_m of Mod1 represents a lower bound on the moulin cross-sectional area. With Mod2 we investigated the influence of a 1.5 times larger S_m on \hat{v}_{main} , showing a pronounced maximum of \hat{v}_{main} during the peak of the flood in phase 2 (14 June, Fig. 6d) which is, according to the above argument, more realistic. Values of S_m used in Mod1 and Mod2 are reasonable estimates for a moulin operating over several years (like M1) and are comparable to the cross-sectional area at the top of the moulin that Piccini and others (2000) explored on Gornergletscher.

We do not have enough data to fit the other free parameters (l_c and n_{man}) of the model, or to constrain the geometry of the moulin better. For this, injections over the whole diurnal discharge cycle (Schuler and others, 2004) and, in particular, during periods of low subglacial water pressure are needed, which would then give better bounds on \hat{v}_{main} . Fitting l_c and n_{man} can pose additional problems, as shown by Werder and Funk (2009).

The maximum \hat{v}_{main} was obtained by estimating the maximum t (Equation (10)). Even this maximum transit speed, $\hat{v}_{\text{main}} = 1.34 \text{ m s}^{-1}$, is low compared to predictions of a jökulhlaup model applied to Gornergletscher. As reported in the companion paper (Werder and Funk, 2009), we ran Clarke's (2003) jökulhlaup model for the first 3 days of the 2006 outburst. At discharges of $18 \text{ m}^3 \text{ s}^{-1}$ (the proglacial discharge measured at maximum \hat{v}_{main} on 14 June 2005 at the time of injection) the calculated flow speed is $2.0\text{--}3.5 \text{ m s}^{-1}$, depending on the model parameters used. Even for discharges of $7 \text{ m}^3 \text{ s}^{-1}$, corresponding to the lake discharge at the injection time, the range of calculated water-flow speed was $1.6\text{--}2.6 \text{ m s}^{-1}$. The comparison, albeit rather

crude as the model is not set up for the 2005 jökulhlaup, shows that the simulated flow speed is larger than \hat{v}_{main} , concurring with the findings of Werder and Funk (2009). This discrepancy may be due to a sinuous channel, an erroneous estimate of maximum t (Equation (10)), or shortcomings of the jökulhlaup model.

Schuler and others (2004) showed that the diurnal variability of transit speed ($0.3\text{--}0.8 \text{ m s}^{-1}$) is due to changes in meltwater flux and can be as great as the variability we found during the jökulhlaups. Werder (2009) shows that most of this diurnal variability is due to changing moulin discharge, but that some is also due to changing subglacial water pressure conditions. By injecting the dye always at the same time of the day, these conditions were kept as constant as possible for different injections, given the changing environment and boundary conditions inherent in all field experiments. This procedure made the results from different injections comparable to each other; however, some of the observed changes could also be due to these other factors and not the jökulhlaup. In 2005, during the injections into M1, the weather conditions were stable, apart from a colder 14 June, so we think that our interpretation of the results is valid. In 2007, the weather was not as stable; however, the doubling of transit speed is a very strong signal and so it is likely that the jökulhlaup contributed significantly. Furthermore, only tracer experiments conducted using the same moulin should be directly compared to one another, as other tracer experiments (not presented here) showed that injections at the same time of the day into different moulins can yield transit speeds that vary by almost an order of magnitude (Werder, 2009). Aschwanden and Leibundgut (1982) conducted a tracer study during the jökulhlaup of Gornersee in 1979. They performed three injections: one before the jökulhlaup, one when the proglacial discharge reached its maximum and one just after. However, they injected at different times of the day using two different moulins, so their results cannot be compared to ours.

During the jökulhlaup, an amount of water equal to half of the lake volume is temporarily stored within the glacier. This can be calculated by integrating the lake discharge minus the additional proglacial discharge due to the lake drainage (Huss and others, 2007). We have clear evidence for water-storage processes from tracer experiments in both 2005 and 2007. On 12 June 2005, in phase 1 of the jökulhlaup, the maximum dispersion, D , and the minimum fraction of mobile water, β , (Fig. 3b and c) were recorded. On this day very turbid water exited from the glacier terminus, and Huss and others (2007) report the onset of storage of lake water within the glacier. This concurrence of maximum D and minimum β was also observed in 2007 (injection into M3 on 10 July; Fig. 4g and h) during one of the intermittent subglacial discharge events in phase 2. Also in 2007, the injection into M3 on 9 July (Fig. 5b) resulted in a M of 0.1, compared to 0.35 throughout the rest of the jökulhlaup (Fig. 4i). The breakthrough curve of that experiment (Fig. 5b) could not be fitted by the ASDM model but it was very broad and thus D was high. These observations suggest that water is stored at the glacier bed by spreading laterally from the channel outwards. This increases turbulent mixing, leading to a higher D , and large amounts of water can access regions which otherwise conduct little discharge and mobilize the sediment there, leading to turbid

water. The water which is spread out laterally will flow slower and thus causes parts of the tracer to be delayed (lower β) and also to be diluted to concentrations too low to detect (lower M).

CONCLUSIONS

When estimating the water transit speed in the main subglacial drainage channel from tracer experiments, the whole flow path of the tracer must be taken into account. We show that tracer retardation in the injection moulin can explain the low measured tracer transit speeds during the peak of the jökulhlaup. To arrive at main drainage channel transit-speed estimates, it was necessary to make some assumptions about the moulin residence time of the tracer. These assumptions could be better constrained if tracer were injected more often, in particular at times of low subglacial water pressure. Our estimates of the main drainage channel transit speeds, where lake water also flows, show that they are low compared to flow speed predictions of a jökulhlaup model. Water-storage processes during jökulhlaups are important, and our observations suggest that they are caused by lateral spreading of the water at the bed.

ACKNOWLEDGEMENTS

The project was funded by the Swiss National Science Foundation, grant Nos. 200021-103882/1 and 200020-111892/1. We are grateful to many members of VAW/ETH Zürich and others who helped with data acquisition, fieldwork and data processing. Grande Dixence SA allowed us to use their infrastructure to install the fluorimeters and provided the discharge data. The Swiss military and the International Foundation High Altitude Research Stations Jungfrauoch and Gornergrat (HFSJG) provided logistical support. M. Schurter lent us his BackScat fluorimeter. M. Huss provided the lake-discharge calculations. We thank H. Horgan, P. Riesen, M. Truffer, M. Huss, S. Braun-Clarke and, in particular, T.V. Schuler for their helpful comments. We also thank an anonymous reviewer, G.K.C. Clarke and scientific editor R. Hock for their numerous and helpful revisions.

REFERENCES

- Anderson, S.P. and 6 others. 2003. Integrated hydrologic and hydrochemical observations of Hidden Creek Lake jökulhlaups, Kennicott Glacier, Alaska. *J. Geophys. Res.*, **108**(F1), 6003. (10.1029/2002JF000004.)
- Aschwanden, H. and C. Leibundgut. 1982. Die Markierung der Wasser des Gornerseeausbruchs mit drei Fluoreszenztracern. *Beitr. Geol. Schweiz*, **28**(11), 535–549.
- Bartholomäus, T.C., R.S. Anderson and S.P. Anderson. 2008. Response of glacier basal motion to transient water storage. *Nature Geosci.*, **1**(1), 33–37.
- Björnsson, H. 1998. Hydrological characteristics of the drainage system beneath a surging glacier. *Nature*, **395**(6704), 771–774.
- Chow, V.T., D.R. Maidment and L.W. Mays. 1988. *Applied hydrology*. New York, McGraw-Hill Inc.
- Clarke, G.K.C. 1996. Lumped-element analysis of subglacial hydraulic circuits. *J. Geophys. Res.*, **101**(B8), 17,547–17,560.
- Clarke, G.K.C. 2003. Hydraulics of subglacial outburst floods: new insights from the Spring–Hutter formulation. *J. Glaciol.*, **49**(165), 299–313.
- De Smedt, F., W. Brevis and P. Debels. 2005. Analytical solution for solute transport resulting from instantaneous injection in streams with transient storage. *J. Hydrol.*, **315**(1–4), 25–39.
- Fisher, D. 1973. Subglacial leakage of Summit Lake, British Columbia, by dye determinations. *IASH Publ.* 95 (Symposium at Cambridge 1969 – *Hydrology of Glaciers*), 111–116.
- Fountain, A.G. 1993. Geometry and flow conditions of subglacial water at South Cascade Glacier, Washington State, USA; an analysis of tracer injections. *J. Glaciol.*, **39**(131), 143–156.
- Fountain, A.G. and J.S. Walder. 1998. Water flow through temperate glaciers. *Rev. Geophys.*, **36**(3), 299–328.
- Fowler, A.C. 1999. Breaking the seal at Grímsvötn, Iceland. *J. Glaciol.*, **45**(151), 506–516.
- Hubbard, B. and P. Nienow. 1997. Alpine subglacial hydrology. *Quat. Sci. Rev.*, **16**(9), 939–955.
- Huss, M., A. Bauder, M. Werder, M. Funk and R. Hock. 2007. Glacier-dammed lake outburst events of Gornersee, Switzerland. *J. Glaciol.*, **53**(181), 189–200.
- Käss, W. 1998. *Tracing technique in geohydrology*. Rotterdam/Brookfield, A.A. Balkema.
- Kohler, J. 1995. Determining the extent of pressurized flow beneath Storglaciären, Sweden, using results of tracer experiments and measurements of input and output discharge. *J. Glaciol.*, **41**(138), 217–231.
- Lang, H., C. Leibundgut and E. Festel. 1981. Results from tracer experiments on the water flow through the Aletschgletscher. *Z. Gletscherkd. Glazialgeol.*, **15**(2), 209–218.
- Nienow, P.W., M.J. Sharp and I.C. Willis. 1996. Velocity–discharge relationships derived from dye tracer experiments in glacial meltwaters: implications for subglacial flow conditions. *Hydrol. Process.*, **10**(10), 1411–1426.
- Nye, J.F. 1976. Water flow in glaciers: jökulhlaups, tunnels and veins. *J. Glaciol.*, **17**(76), 181–207.
- Piccini, L., A. Romeo and G. Badino. 2000. Moulins and marginal contact caves in the Gornergletscher, Switzerland. *Nimbus* 23–24, 94–99.
- Roberts, M.J. 2005. Jökulhlaups: a reassessment of floodwater flow through glaciers. *Rev. Geophys.*, **43**(1), RG1002. (10.1029/2003RG000147.)
- Röthlisberger, H. 1972. Water pressure in intra- and subglacial channels. *J. Glaciol.*, **11**(62), 177–203.
- Schuler, T. and U.H. Fischer. 2003. Elucidating changes in the degree of tracer dispersion in a subglacial channel. *Ann. Glaciol.*, **37**, 275–280.
- Schuler, T., U.H. Fischer and G.H. Gudmundsson. 2004. Diurnal variability of subglacial drainage conditions as revealed by tracer experiments. *J. Geophys. Res.*, **109**(F2), FO2008. (10.1029/2003JF000082.)
- Spring, U. and K. Hutter. 1982. Conduit flow of a fluid through its solid phase and its application to intraglacial channel flow. *Int. J. Eng. Sci.*, **20**(2), 327–363.
- Stearns, L.A., B.E. Smith and G.S. Hamilton. 2008. Increased flow speed on a large East Antarctic outlet glacier caused by subglacial floods. *Nature Geosci.*, **1**(12), 827–831.
- Sugiyama, S., A. Bauder, P. Weiss and M. Funk. 2007. Reversal of ice motion during the outburst of a glacier-dammed lake on Gornergletscher, Switzerland. *J. Glaciol.*, **53**(181), 172–180.
- Sugiyama, S., A. Bauder, M. Huss, P. Riesen and M. Funk. 2008. Triggering and drainage mechanisms of the 2004 glacier-dammed lake outburst in Gornergletscher, Switzerland. *J. Geophys. Res.*, **113**(F4), F04019. (10.1029/2007JF000920.)
- Toride, N, F.J. Leij and M.Th. van Genuchten. 1999. *The CXTFIT code for estimating transport parameters from laboratory or field tracer experiments. Version 2.1*. Riverside, CA, US Department of Agriculture. US Salinity Laboratory. (Research Report 137.)

- Tweed, F.S. and A.J. Russell. 1999. Controls on the formation and sudden drainage of glacier-impounded lakes: implications for jökulhlaup characteristics. *Progr. Phys. Geogr.*, **23**(1), 79–110.
- Van Genuchten, M.T. and P.J. Wierenga. 1976. Mass transfer studies in sorbing porous media: I. Analytical solutions. *Soil Sci. Soc. Am. J.*, **40**(4), 473–480.
- Walter, F., N. Deichmann and M. Funk. 2008. Basal icequakes during changing subglacial water pressures beneath Gornergletscher, Switzerland. *J. Glaciol.*, **54**(186), 511–521.
- Walter, F., J.F. Clinton, N. Deichmann, D.S. Dreger, S.E. Minson and M. Funk. In press. Moment tensor inversions of icequakes on Gornergletscher, Switzerland. *Bull. Seismol. Soc. Am.*, **99**(2A), 852–870.
- Werder, M.A. 2009. Dye tracing and modelling jökulhlaups. (PhD thesis, ETH Zürich.)
- Werder, M.A. and M. Funk. 2009. Dye tracing a jökulhlaup: II. Testing a jökulhlaup model against flow speeds inferred from measurements. *J. Glaciol.*, **55**(193), 899–908.

MS received 30 August 2008 and accepted in revised form 7 September 2009